Chemistry–A European Journal
Research Article
doi.org/10.1002/chem.202400120
Chemistry Europe
European Chemical Societies Publishing
www.chemeurj.org

Synthesis of N-Glycosylated Soluble Fas Ligand

Alanca Schmid,[a] Claudia Bello,[b] and Christian F. W. Becker*[a]

Controlled cell death is essential for the regulation of the immune system and plays a role in pathogen defense. It is often altered in pathogenic conditions such as cancer, viral infections and autoimmune diseases. The Fas receptor and its corresponding membrane-bound ligand (FasL) are part of the extrinsic apoptosis pathway activated in these cases. A soluble form of FasL (sFasL), produced by ectodomain shedding, displays a diverse but still elusive set of non-apoptotic functions and sometimes even serves as a pro-survival factor. To gather more knowledge about the characteristics of this protein and the impact N-glycosylations may have, access to homogeneous posttranslationally modified variants of sFasL is needed. Therefore, we developed a flexible strategy to obtain such homogeneously N-glycosylated variants of sFasL by applying chemical protein synthesis. This strategy can be flexibly combined with enzymatic methods to introduce more complex, site selective glycosylations.

Introduction

The Fas receptor (also called APO-1 or CD95)[1] and its corresponding ligand (FasL/CD95L/Apo-1 ligand)[2] are the best understood death receptor/ligand system up to now.[3] FasL is a transmembrane protein expressed on activated T-cells, natural killer cells and immune privileged tissue[4] while the corresponding receptor (Fas) is ubiquitously expressed in various tissues. Binding of FasL causes the Fas receptor to recruit FADD[5] and in turn activates procaspases 8 and 10,[6] forming the so called death-inducing-signaling-complex (DISC).[7] Subsequently, several caspases get activated, culminating in the apoptosis of the receptor containing cell.[8] This extrinsic apoptosis pathway plays an important role in T-cell regulation and cancer progression.[8b,9]

Structurally FasL consists of an intracellular part with a proline-rich domain (PRD) and a casein kinase I substrate motive (CSM), a transmembrane domain and an extracellular fragment (Scheme 1).[10] Ectodomain shedding mediated by the ADAM10 protease can release a 151 to 154 amino acid protein segment, acting like a cytokine, into the extracellular space. This segment is called soluble Fas ligand (sFasL).[11] Cleavage by other metalloproteinases (MMP3, MMP7, MMP9) leads to different soluble cytokines with distinct apoptosis-mediating properties.[12]

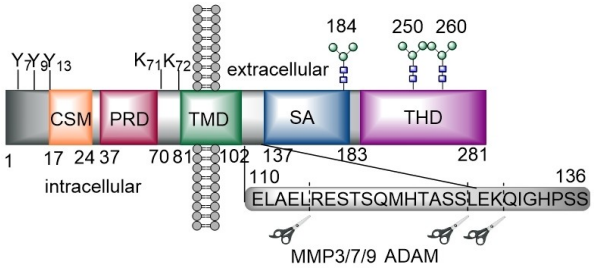

Scheme 1. Domain structure of FasL. CSM = casein kinase substrate motive, PRD = proline-rich domain, TMD = transmembrane domain, SA = self-assembling domain, THD = TNF homology domain. MMP = matrix metalloproteinase, ADAM = A disintegrin and metalloproteinase domain, 110–136 = stalk region. Position 184/250/260 = N-glycosylation sites. Position 7/9/13 = phosphorylation sites (Y). Position 71/72 = ubiquitylation sites (K).

sFasL exhibits a very low ability to induce apoptosis,[13] suggesting that proteolytic cleavage is a mechanism of down-regulating the killing activity.[13–14] However, other data suggest that the non-apoptotic signaling of sFasL and the apoptotic signaling of FasL both have to act synergistically to achieve the most potent killing activity.[15] In 1998, Schneider *et al.* could show that the reduced ability to induce apoptosis by sFasL is connected to its inability to form multi-aggregated trimers.[13] On the other hand, sFasL binding can lead to expression and secretion of cytokines such as interleukin (IL) 2, promoting further T-cell proliferation and inflammation.[16] sFasL also seems to play a role in angiogenesis probably by stimulating vascular endothelial growth factor (VGFR) in cancer tissue.[15a,17] In general, Fas/FasL interaction does not only induce apoptosis but can lead to the production of cytokines as well as anti-apoptotic factors, making Fas/FasL a highly relevant but complex target for immuno-oncology research.[18]

Inhibiting Fas/FasL signaling is a viable concept used by the drug asunercept, a fusion protein consisting of the extracellular part of Fas receptor fused to the Fc region of an IgG1 antibody,[19] which is approved for the treatment of graft-

[a] *Dr. A. Schmid, Prof. Dr. C. F. W. Becker*
Institute of Biological Chemistry
Faculty of Chemistry, University of Vienna
Währinger Straße 38, 1090, Vienna Austria
E-mail: christian.becker@univie.ac.at
Homepage: https://biologischechemie.univie.ac.at/

[b] *Prof. Dr. C. Bello*
Interdepartmental Research Unit of Peptide and Protein Chemistry and Biology, Department of Chemistry "Ugo Schiff"
University of Florence
Via della Lastruccia 13, 50019 Sesto Fiorentino FI, Italy

Supporting information for this article is available on the WWW under https://doi.org/10.1002/chem.202400120

versus-host disease (2006), glial tumor (2010) and myelodysplastic syndrome (2017) in the European Union.[19] Also recently, different groups could show that plasma levels of sFasL correlate with disease severity in COVID-19 patients.[20] Low sFasL plasma levels and increased Fas receptor expression seem to strongly intensify neutrophil necroptosis, leading to an inflammation feedback loop, impacting disease severity.[20a,21]

To date the factors which influence the transformation of FasL into sFasL and the resulting physiological consequences are not fully understood. Synthetic access to sFasL variants would be desirable, especially since posttranslational modifications such as N-glycosylation increase its structural and functional diversity beyond direct genetic control.[22] So far only small amounts of recombinantly expressed sFasL variants have been available, due to low expression levels and the challenging properties of this proteins with respect to solubility and oligomerization.[23] Here, we set out to establish synthetic access to homogeneously N-glycosylated sFasL variants using an approach that links three synthetic peptides to obtain full-length sFasL and enables further chemoenzymatic glycosylation (Scheme 2 & SI for details on glycan synthesis).

Results and Discussion

Since sFasL lacks any suitably placed cysteine residues around the C-terminal ligation site for native chemical ligation (NCL, see Scheme S1), we chose to adapt an approach developed by Bello *et al.*[24] and introduced a ligation mediating, PEGylated auxiliary at the N-terminus of the C-terminal peptide sFasL 247–281 to make use of an X-Gly ligation site (**4**). This strategy not only enables ligations at X-glycine junctions but also increases peptide solubility due to the attached PEG moiety. To incorporate site specifically placed homogeneous N-glycans that have been found in native sFasL,[25] Asn-GlcNAc building blocks were introduced into sFasL-A^{247}-L^{281} at positions 250 and/or 260 (**4**).

We envisioned that these synthetically incorporated GlcNAc residues could give rise to more complex N-glycans by transferring an oxazoline activated N-glycan core structure (tetrasaccharide generated from egg yolk) *en bloc* using endoglycosynthases (hydrolysis-inhibiting mutants of endoglycosidases, Scheme S2).[26] Glycosyltransferases could subsequently be used to elongate the carbohydrate chain allowing the synthesis of different N-glycan variants.[24]

The synthesis of sFasL-K^{141}-Q^{201}-NHNH$_2$ (**1a**) and sFasL-C^{202}-L^{245}-NHNH$_2$ (**2**) by SPPS on a Tentagel® resin followed by hydrazinolysis[27] (**1a**) or directly on a hydrazide-2-CTC resin (**2**), proceeded smoothly and yielded the peptides with C-terminal hydrazides as thioester precursors (Figure S1, Figure S3). sFasL-K^{141}-Q^{201}-NHNH$_2$ **1a** was converted to the corresponding MesNa thioester **1b**, following the protocol from Zheng *et al.*[28] (Figure S2).

NCL of **1b** with **2** gave ligation product **3a** in 13% isolated yield. The rather low yield resulted from overlapping elution of product **3a** and peptide **1b** with hydrolyzed thioester (Figure S4). After conversion of **3a** into C-terminal thioester peptide **3b**, a second charge series appeared that corresponds to a loss of the thioester (Figure S5). At this point, we suspected formation of a thiolactone by reaction of the C-terminal thioester with one of the two internal cysteines (Cys^{202} or Cys^{233}). However, the resulting cyclic peptide thiolactone should still be reactive in NCL reactions and was carried forward.

Peptide aglycone **4a** and its glycosylated variants containing AsnGlcNAc building blocks at positions 250 and/or 260 (**4b/c/d**) were synthesized manually (Figure S6-S9). Based on experience with synthesizing the non-glycosylated peptide segment, we included Leu-Ser/Leu-Thr isoacyl dipeptide build-

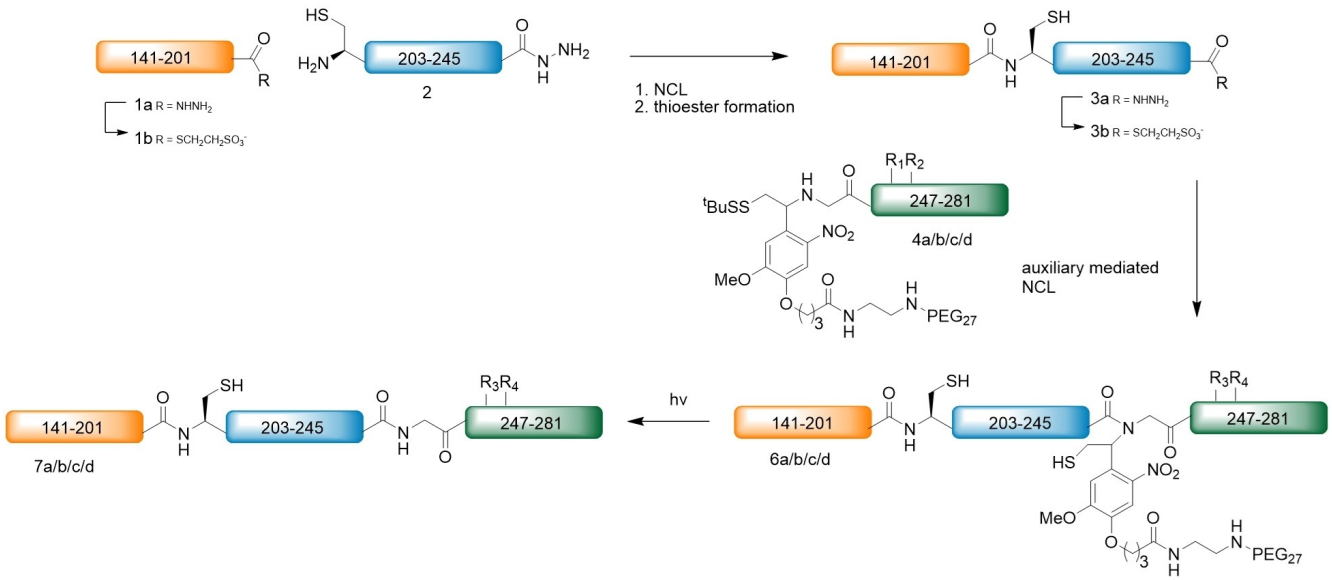

Scheme 2. A) Schematic overview of synthetic steps to obtain homogeneously glycosylated sFasL-K^{141}-L^{281} variants using a ligation and solubilization mediating auxiliary at the N-terminus of sFasL-A^{247}-L^{281} as described by Bello *et al.*[24]

ing blocks (at positions 251–252/264-265, Scheme S1) to prevent aggregation during the synthesis as well as enhancing solubility for purification.[29] Finally, the auxiliary was attached to the N-terminus, PEGylated and the peptides were cleaved from resin. Subsequently, peptides containing isoacyl building blocks (**4 b/c/d**) were dissolved in 6 M urea at pH 8 to restore the native amide bonds between Leu-251 and Ser-252 and between Leu-264 and Thr-265 and the acetyl protecting groups of the carbohydrate moiety were removed by treatment with sodium methoxide (NaOMe). The resulting fully deprotected (glyco)peptide conjugates were purified by HPLC (Figure S6-S9) and used in the auxiliary-mediated ligation with **3 b** (Scheme 2). Unfortunately, when subjecting peptides **4 a/b** and **3 b** to NCL conditions no product could be detected and the previously observed thiolactone remained stable under NCL conditions. Screening a large variety of conditions (with varying additives, temperatures, pHs and concentrations) did not improve this result (Table S1). Low solubility of peptide segments in combination with the sterically hindered secondary amine involved in the S-to-N acyl shift as well as the very stable thiolactone most likely prevented a successful ligation.[30] At the same time, we could confirm thiolactone formation in peptide **3** with both Cys202 and Cys233, which was efficiently prevented by protecting cysteine side chains (Figure S10-S12).

Since we were unable to optimize reaction conditions, we decided to change our approach towards the more reactive diselenide-selenoester ligation (DSL) instead of auxiliary-mediated ligation to accelerate the ligation reaction. DSL is indeed expected to enhance reaction rates even at difficult junctions and at much lower concentrations.[31] Moreover, we introduced a novel photocleavable linker on the side chain of a glutamic acid, as recently described by Kerul *et al.*,[32] that we further modified to attach two PEG_{27} chains for enhanced solubility (Scheme 3, left, **10 a/b/c/d**). This new approach required a slight shift in the ligation site and the synthesis of two new peptide segments (**8** & **10 a/b/c/d**, Scheme 3). Ala247 was changed to selenocysteine as it can be selectively converted to alanine after ligation in the presence of unprotected cysteine, recovering the native sequence.[33] Peptide **8** was accessed smoothly (Figure S10) and peptides **10 a/b/c/d** (sFasL-U^{247}-E^{273}(AuxLys2xPEG)-L^{281}) were also successfully synthesized (Figure S13-S17). A remarkable increase in the solubility of **10 a/b/c/d** was observed

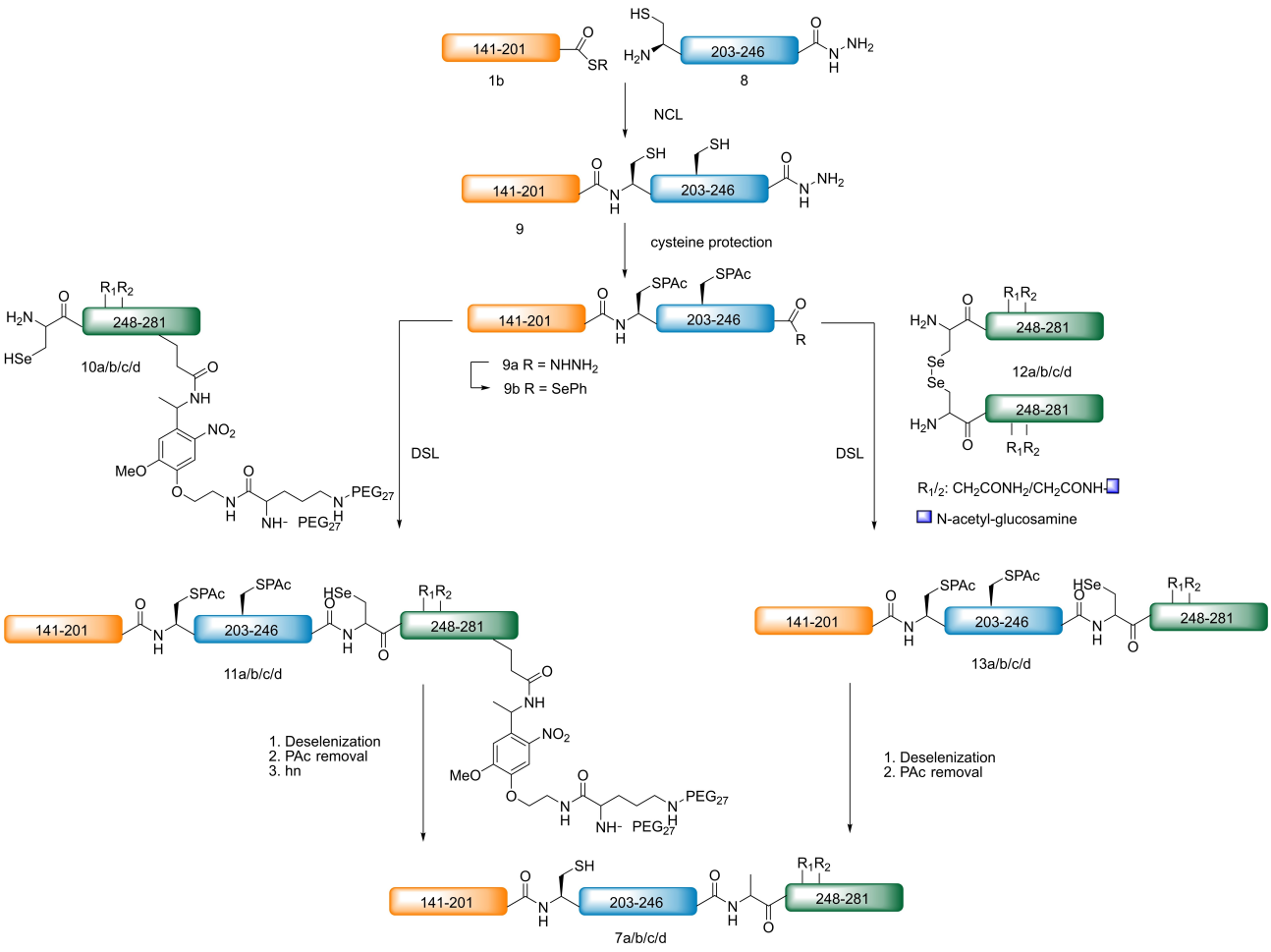

Scheme 3. Left: Synthetic strategy to obtain **7** using solubilization tag ($2xPEG_{27}$) attached to a glutamic acid sidechain *via* a photocleavable structure described by Kerul *et al.*[35] (**10 a/b/c/d, 11 a/b/c/d**). Right: Synthetic strategy to obtain **7** without using any solubilization tag but working at micromolar concentrations for DSL reaction (**12 a/b/c/d, 13 a/b/c/d**). **7/10/11/12/13 a**: aglycon, **7/10/11/12/13 b**: glycosylated at position 250, **7/10/11/12/13 c**: glycosylated at position 260, **7/10/11/12/13 d**: glycosylated at position 250 + 260.

compared to **4a/b/c/d** due to the diPEGylated linker. After NCL between sFasL-K^{141}-Q^{201} (**1b**) and sFasL-C^{202}-G^{246} (**8**) to give sFasL-K^{141}-G^{246} (**9**) we protected both cysteine residues with phenacyl (PAc) protecting groups to avoid formation of the thiolactone (Figure S18, **9a**). PAc protection was cleanly achieved with a protocol previously established in our group.[34]

We directly accessed peptide-selenoester **9b** (Figure 1) from peptide hydrazide **9a** in PAc protection solution. With **9b** and **10b** in hand, DSL reactions and subsequent deselenization proceeded smoothly, giving rise to deselenized **11b** (Figure S20-S21). To maintain the solubilizing effect provided by AuxLys2xPEG, PAc removal was carried out next. However, conditions used for PAc removal from cysteine side chains (zinc, AcOH[34b]) reduced the nitro group at the solubilization tag to an amine, preventing subsequent photocleavage (Figure S22). Removing the solubilization tag prior to the PAc groups led to complete precipitation of the protein.

Based on these challenges, we decided to circumvent the large variety of available solubilization tags,[36] which almost always require an additional cleavage step, by pursuing a combination of cysteine PAc protection of **9** (to prevent thiolactone formation) and DSL with **12a/b/c/d** at micromolar concentrations (Scheme 3, right).

Peptide diselenides **12a/b** were synthesized by standard Fmoc-SPPS. After global deprotection, the GlcNAc acetyl protecting groups were removed by incubating the lyophilized peptide in a small amount of 6 M GdnHCl at pH 9 for 5 minutes. Transprotection of the selenol-protecting group from Mob to Npys was performed without further purification by adding 25 eq. 2,2′-dithiobis(5-nitropyridine) (DTNP) in 96% TFA, 2% DMS and 2% thioanisole (1:20) for 1 hour. After precipitation in cold diethyl ether and lyophilization, the peptide was dissolved in 6 M GdnHCl containing 100 mM DTT and 100 mM ammonium bicarbonate at pH 6 (10 minutes) to remove the Npys group and to form the peptide diselenides **12a/b** (**12a** see Figure S23). After HPLC purification, peptide **12b** was obtained in 12% yield based on the crude material used for deprotection reactions (Figure 2). The low signal-to-noise ratio in the mass spectrum of **12b** is a result of low peptide solubility and poor ionization of selenium-containing peptides.[30c]

DSL reactions with **12b** and **9b** following the protocol from Kulkarni *et al.*[31c] led to unreactive Npys diselenides, which prevented effective ligation under these conditions. Furthermore, peptide **12b** was only soluble at slightly higher pH due to a pI of around 4.4.[37] Therefore, we adapted a protocol from Chisholm *et al.*[31d] by slightly increasing the pH (5.1 to 5.8) and adding only 4 eq. of pre-reduced phenylselenol instead of mM concentrations. Peptide **9b** was dissolveed in ligation buffer, peptide **12b** and 4 eq. of pre-reduced phenylselenol were added and the mixture was incubated at 37 °C for 30 minutes.

Without further purification, DPDS was extracted with hexane (to prevent inhibition of deselenization) and the mixture was diluted 1:1 with deselenization buffer under argon for approximately 5 hours at rt. Figure 3 shows the HPLC chromatogram of the deselenization mixture and a MS spectrum of the desired product **7'b** (peak at 13.4 minutes). Without purification, the PAc protecting groups were removed by adding zinc/AcOH to the solution. Fully deprotected sFasL-K^{141}-L^{281} (**7b**) was purified and analyzed by HPLC and MS (Figure 3, data for non-glycosylated version **7a** can be found in Figure S23). Both variants were obtained in low to medium yields, e.g. 1 mg of **7a** was prepared from roughly 5 mg of starting peptide segments **1b**, **8** and **12a**.

As the detected mass of **7b** suggests an already oxidized product, DTT was added before folding was started either by dialysis or dilution. After folding both by dilution and dialysis, monomeric, water soluble, site-specifically N-glycosylated sFasL

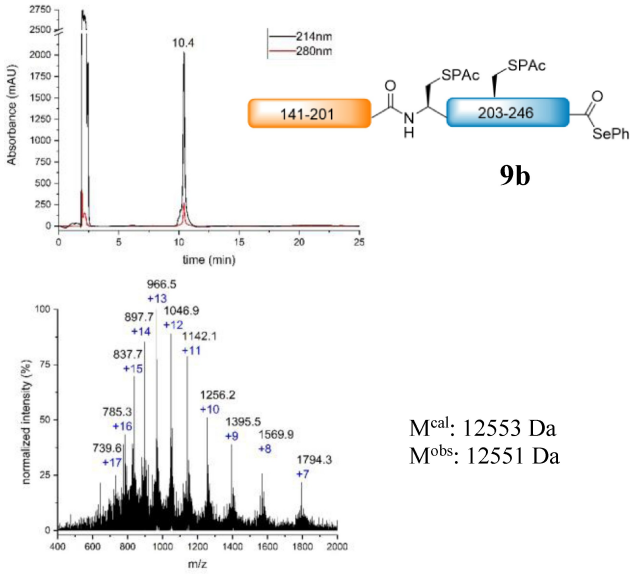

Figure 1. HPLC chromatogram (45–55% B in 7 minutes, 60 °C) and corresponding mass spectrum of compound **9b**. M^{cal} = calculated mass, M^{obs} = observed mass.

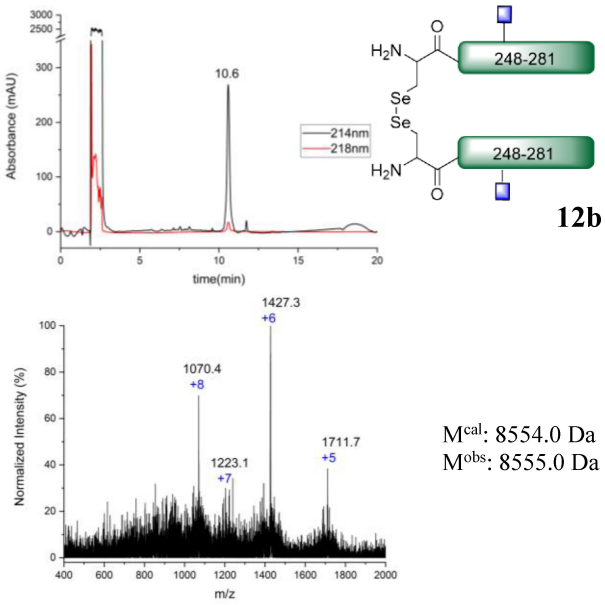

Figure 2. HPLC chromatogram (45–55% B in 7 minuntes, 60 °C) and mass spectrum of compound **12b** dimer. M^{cal} = calculated mass, M^{obs} = observed mass.

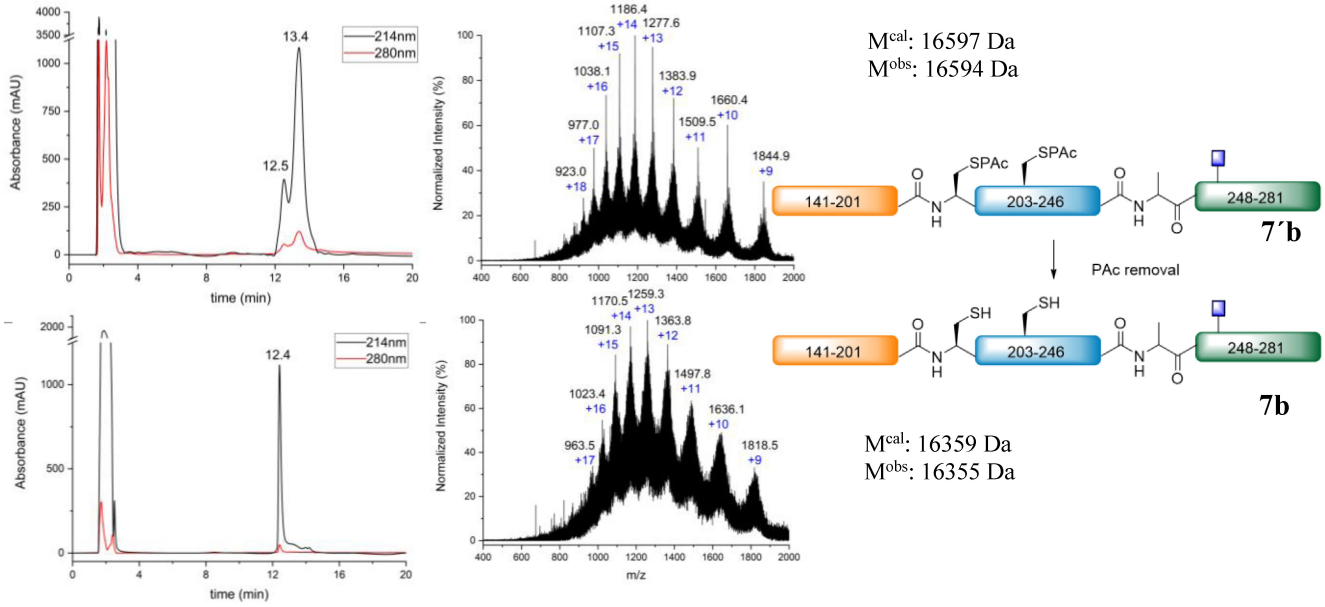

Figure 3. HPLC chromatogram (45–65% B in 14 minutes) and corresponding high-resolution mass spectrum of deselenization mixture (peak at 12.5 minutes: hydrolyzed **9**, peak at 13.4 minutes: **7'b**) and final product **7b** after PAc removal and purification, analyzed with formic acid containing buffers. M^{cal} = calculated mass, M^{obs} = observed mass.

7b was obtained. The corresponding CD spectrum indicates a predominantly β-sheet rich secondary structure (Figure S24).

Conclusions

Accessing homogeneously glycosylated sFasL-K^{141}-L^{281} turned out to be highly challenging, mainly due to solubility issues and oligomerization of peptide segments. Low solubility in aqueous buffers made it difficult to purify peptide segments and to perform ligation reactions at concentrations required for NCL to work efficiently. This was also, in part, the reason why auxiliary mediated ligations were not effective. These reactions also suffered steric hindrance that slowed down the reaction to an extent where no product formation could be observed, especially in competition with hydrolysis and thiolactone formation. The latter was observed for peptide **3** and **9** after C-terminal activation. Only protection of cysteine thiol groups could prevent this reaction, which unfortunately interfered with conditions used to remove the photocleavable solubilization tag. Eventually, we succeeded with this ligation reaction employing a diselenide-selenoester ligation (DSL), since this reaction can be performed even at nanomolar concentrations,[31d] the solubility especially of the C-terminal peptide without any solubilization tag (**12a/b**) was still sufficient to convert the educts to the desired products **13a/b**.

We were able to synthesize sFasL-K^{141}-L^{281} containing a site selectively placed AsnGlcNAc, which can be further glycosylated as depicted in scheme S2 in a flexible combination with chemoenzymatic methods. Although we were able to obtain a suitable N-glycan oxazoline for enzymatic transfer (scheme S2 **5c**), suitable reaction conditions have to be found for the transfer to this specific target protein.

To the best of our knowledge, this is the first time sFasL-K^{141}-L^{281} has been fully synthesized and site selectively modified, providing access to this enigmatic soluble variant of the Fas ligand for detailed biochemical analysis and potential therapeutic applications in immune-oncology and infection biology.

Experimental Section

Peptide Synthesis

Solid phase peptide synthesis was carried out following standard Fmoc-based SPPS protocol.[38] If not stated otherwise, N-terminally Fmoc-protected L-amino acids and pseudoproline dipeptides with standard protecting groups (SI) and pre-loaded, low loading Tentagel resins were used. To increase the coupling yield, amino acids in certain positions (SI) were double coupled, meaning the coupling procedure was repeated without removing the Fmoc group in between.

Manual SPPS

For manual synthesis 5 eq. amino acid, 5 eq HATU and 6 eq DIPEA were used and the coupling was performed for 15 minutes. Fmoc deprotection was achieve by incubating the resin 2x5 minutes in 20% piperidine in DMF. Fmoc-L-Asn($(Ac)_3$-β-D-GlcNAc)-OH was only used in 2-fold excess and coupled for 30 minutes. Since Sec is sensitive to basic conditions, for the coupling of Fmoc-Sec(Mob)-OH (2 h) and all following coupling steps (30 min), 4 eq. aa, 4 eq. Oxyma and 4.4 eq. DIC were used. Boc-L-Ser(Fmoc-L-Leu)-OH and Boc-L-Thr(Fmoc-L-Leu)-OH isoacyl dipeptide were coupled using the same condition as for Sec-containing peptides described above.

Automated SPPS

Automated peptide synthesis was performed on a microwave-assisted Liberty Blue system from CEM (10 eq. amino acid, 10 eq. Oxyma (+0.4 eq. DIPEA if modified 2-CTC resin was used), 10 eq. DIC) or the PTI Tribute synthesizer (Protein Technologies, Inc.) (5 eq. amino acid, 5 eq. HBTU, 5 eq. DIPEA).

Cleavage

After the synthesis was completed, the resins were washed with DCM and dried in the desiccator. To remove side chain protecting groups and release the peptide, the peptidyl resin was incubated in 90% TFA, 5% DMS, 2.5% H_2O and 2.5% TIPS for 3 hours. After precipitation in cold diethyl ether and centrifugation, the residue was dissolved in 80% ACN in H_2O and lyophilized.

Hydrazide generation

Stable hydrazides were used as thioester surrogates and further activated *via* sodium nitrite and a thiol component as described by Zheng *et al.*.[28] To generate them, two strategies were applied: using a modified 2-clorotrityl chloride (2-CTC) resin containing a hydrazide linker[28] or SPPS on a standard Tentagel® resin and subsequent hydrazinolysis.[27]

For linker preparation, 500 mg 2-CTC resin from ChemImpex were used (Loading: 1.45 mmol/g). The resin was washed with DMF/DCM (3x5 mL DMF, 3×5 mL DCM, 3×5 mL DMF). Subsequently, a mixture of DMF/DCM (1:1, 5 mL) was added and the resin was swelled for 30 minutes. The solvent was drained, a solution of $NH_2NH_2{\times}H_2O$ (12.5 mL, 10 vol % hydrazine monohydrate in DMF) was added and the resin was agitated for 30 minutes at room temperature. After washing once with DMF, the hydrazine incubation was repeated. Afterwards, the resin was thoroughly washed three times with DMF/DCM (see above). Unreacted functional groups were capped by agitating the resin in MeOH/DMF (12.5 mL, 5 vol % MeOH in DMF) for 20 minutes. The resin was washed with DMF, DCM and DMF (3×5 mL, respectively) dried and the loading was determined by photometric Fmoc quantification. The resin was directly used for coupling of the C-terminal amino acid. To reduce the loading a 1:1 mixture Fmoc and Boc protected amino acid was used.

For hydrazinolysis on Tentagel, the dried resin was incubated in 1 M hydrazine in THF for 5 h. Since the protected peptides were cleaved but still remained associated with the resin after draining the supernatant (sFasL-K^{141}-L^{201}), the resin was washed with THF, dried and incubated in cleavage solution to remove side chain protecting groups and release the peptide from the resin.

Thioester generation

To convert the C-terminal hydrazides to thioesters, a protocol from Zheng *et al.*[28] was adapted. Therefore, purified peptide was dissolved in buffer containing 6 M GdnHCl and 0.2 M sodium phosphate pH 3 (peptide concentration: 1.2 mM) and the mixture was cooled to −15 °C using an ice/NaCl mixture. To activate the hydrazide by forming an azide, 4.7 eq. $NaNO_2$ (2 mg/ml in H_2O) were added and the mixture was stirred for 20 minutes. The mixture was brought to room temperature, 40 eq. of MesNa in 6 M GdnHCl, 200 mM sodium phosphate pH 3 were added, the pH was set at 6.8 and the mixture was stirred for 15 minutes. Afterwards the thioester was desalted by SEC.

Selenoester generation

Selenoesters were produced from C-terminal hydrazides according to Li *et al.* and Kulkarni *et al.*.[39] Therefore, a 0.25 mM peptide hydrazide solution was prepared by diluting the PAc protection mixture 1:1 with 200 mM TCEP and 100 mM DPDS in 6 M GdnHCl. The pH was set at 1.5 and 25-30 eq. acac were added to start the reaction. The mixture was stirred for 1 h at room temperature. Subsequently DPDS was removed by hexane extraction (three to five times, approximately 1/2 of the original volume hexane was added, shaken for 1 minutes, centrifuged and removed) and the peptide was purified by preparative HPLC.

NCL/DSL

NCL

For native chemical ligation reactions, peptides were dissolved in degassed buffer (6 M GdnHCl, 0.2 M sodium phosphate, 200 mM MPAA, 50 mM TCEP, pH 6.8) obtaining concentrations of 1.6-1.7 mM (cysteine peptide) and 1.4-1.6 mM (thioester peptide). The mixture was stirred at room temperature and reaction progress was monitored by taking timepoints (2 µl sample, diluted with 20 µl 6 M GdnHCl pH 4.7) and subsequent analysis by LC-MS.

DSL and deselenization

Selenocysteine containing peptide was dissolved in 6 M GdnHCl and 200 mM bis-Tris, pH 5.8 (c = 250 µM). Subsequently, selenoester peptide (c = 190 µM) and 4 eq. pre-reduced phenylselenol were added. To create phenylselenol, 5 mg DPDS (16.13 µmol) + 4.15 mg TCEP (14.52 µmol) were incubated in 250 µl 6 M GdnHCl and 200 mM bis-Tris and sonicated for 15 minutes. The mixture was incubated at 37 °C and ligation progress was monitored by LC-MS. Without further purification, DPDS was extracted with hexane (to prevent inhibition of deselenization) and the mixture was subjected to deselenization by diluting it 1:1 with 250 mM TCEP and 25 mM DTT in 6 M GdnHCl, pH 6 and incubating it under argon for approximately 5 hours at rt.

Protecting group introduction and removal

Mob and acetyl protecting group removal

The GlcNAc acetyl protecting groups were removed by incubating the lyophilized peptide in a small amount of 6 M GdnHCl pH 9 for 5 minutes. Transprotection of Mob to Npys was performed one-pot by strongly diluting the mixture (approximately 1:20) with 25 eq. DTNP in 96% TFA, 2% DMS and 2% thioanisole and incubating it for one hour. Subsequently, the peptide was precipitated in cold diethyl ether, centrifuged, the pellet was dissolved in 80% ACN and lyophilized. The lyophilized peptide was dissolved in 100 mM DTT and 100 mM ammonium bicarbonate in 6 M GdnHCl pH 6 for 10 minutes to remove the Npys group and directly purified by RP-HPLC.

PAc protection and removal

For PAc protection, a protocol from Matveenko *et al.* was applied.[34b] Therefore, the peptide was dissolved in degassed 6 M GdnHCl and 0.2 M sodium phosphate, pH 7.2 (0.5 M). Subsequently, 5 eq. PAcBr (0.1 M in DMF) were added and the mixture was stirred at rt for 1 h.

To remove the PAc groups, the mixture after deselenization was diluted with AcOH to obtain a final concentration of 40% AcOH and degassed. 180 mg/ml zinc powder were added and the mixture was incubated for 1 h at rt. Residual zinc was removed by centrifugation, the pellet was washed again with 6 M GdnHCl and the combined solution was diluted to achieve an AcOH concentration of <10%. The peptide was purified by HPLC.

Folding

Dilution

37 μM stock solution of reduced **7** (0.6 mg/ml) in 6 M GdnHCl and 50 mM phosphate at pH 7.5 was prepared. Under constant stirring at 4 °C, the mixture was diluted stepwise with 50 mM phosphate buffer pH 7.5 until a concentration of 0.1 mg/ml was reached. Therefore, the following additions of 50 mM phosphate buffer to 167 μl solution were performed: 20 μl, 30 minutes, 20 μl, 30 minutes, 30 μl, 30 minutes, 50 μl, 30 minutes, 80 μl, 30 minutes, 132 μl, 30 minutes, 500 μl, 30 minutes.

Dialysis

0.1 mg peptide **7** were dissolved in 500 μl 6 M GdnHCl (0.2 mg/ml) + 50 mM Tris at pH 8 and filled into a D-Tube™ Dialyzer Mini, MWCO 6-8 kDa. The dialysis was started against 500 ml 6 M urea, 50 mM Tris, 3 mM DTT, pH 8 for 30 minutes. The following additions to the buffer led to a final concentration of 1 M urea in the peptide containing buffer: 500 ml 6 M urea, 50 mM Tris, pH 8, 30 minutes +100 ml 50 mM Tris, 2 mM GSH, 0.4 mM GSSH, pH 8, 1. 5 h. +250 ml 50 mM Tris, 2 mM GSH, 0.4 mM GSSH, pH 8, 1.5 h. +250 ml 50 mM Tris, 2 mM GSH, 0.4 mM GSSH, pH 8, 1.5 h. +400 ml 50 mM Tris, 2 mM GSH, 0.4 mM GSSH, pH 8, 1.5 h.

Purification and analysis

Preparative HPLC

Peptides were purified on a Varian ProStar instrument using C4 columns from Kromasil. Semipreparative scale purifications (2-20 mg): 10×250 mm 5 μm particle size, flowrate = 3 ml/min. Preparative scale purifications (15-50 mg): 21.2×250 mm 5 μm particle size, flowrate = 10 ml/min. Different gradients of the following solvents were used and all runs were performed at 60 °C: solvent B (ACN + 0.08% TFA), solvent A (H_2O + 0.1% TFA).

Analytical HPLC

Analytical scale purifications (up to 1 mg) and analyses were performed on a Dionex Ultimate 3000 instrument using 4.6×100 mm C4 columns from Kromasil and a flow of 1 ml/min. Different gradients and temperatures were used.

(LC−)-MS

Analytical electrospray ionization mass spectrometry (ESI-MS) was performed on a Waters AutoPurification HPLC/MS System (3100 Mass Detector, 2545 Binary Gradient Module, 2767 Sample Manager and 2489 UV/Visible Detector) either with a prior HPLC separation or as direct injections operating in positive ion mode. In case of very small amounts and/or poor ionization, an LTQ Orbitrap Velos (Mass range: m/z 50-2000 and m/z 200-4000. Resolution: max. >100000 at m/z 400. Mass accuracy: <3 ppm (external) and <1 ppm (internal)) coupled to an UltiMate 3000 RSLCnano system from Thermo Scientific was used. Formic acid instead of TFA enhanced ionization.

Abbreviations

2-CTC: 2-clorotrityl-chloride, acac: acetylacetone, ACN: acetonitrile, ADAM protease: a disintegrin and metalloproteinase, AICD: activation induced cell death, Akt: protein kinase B, BH3: Bcl homology 3 domain, BID: BH3 interacting domain death agonist, Bis-Tris: bis(2-hydroxyethyl)amino-tris(hydroxymethyl)methane, Boc: tert-butyloxycarbonyl, BSA: bovine serum albumin, CDMBI: 2-Chloro-1,3-dimethyl-1H-benzimidazol-3-ium chloride, c-FLIP: cellular FLICE inhibitory protein, CSM: casein kinase I substrate motive, DCM: dichloromethane, DD: death domain, DED: death effector domain, DIC: diisopropylcarbodiimide, DIPEA: diisopropylamine, DISC: death inducing signaling complex, DMF: dimethylformamide, DMS: dimethylsulfide, DPDS: diphenyldiselenide, DSL: diselenide-selenoester ligation, DTNP: dithionitropyridine, DTT: dithiothreitol, EGFR: epidermal growth factor receptor, EMT: epithelial/mesenchymal transition, endo: endoglycosidase, ENGase: endo-β-N-acetylglucosaminidase, ESI-MS: electrospray ionization mass spectrometry, FADD: Fas associated protein with death domain, FasL: Fas ligand, FLICE: caspase 8, Fmoc: fluorenylmethoxycarbonyl, GlcNAc: n-acetyl glucosamine, GM-CSF: granulocyte/macrophage colony-stimulating factor, HATU: 1-[bis(dimethylamino)methylene]-1H-1,2,3-triazolo[4,5-b]pyridinium 3-oxid-hexafluorophosphate, HPLC: high-performance liquid chromatography, IL: interleukine, LC–MS: liquid chromatography mass spectrometry, MesNa: mercaptoethanesulfonic acid sodium salt, MISC: motility-inducing signaling complex, MMP: matrix metalloprotease, Mob: methoxybenzyl, MPAA: mercaptophenylacetic acid, MVB: multivesicular bodies, NADPH: nicotinamide adenine dinucleotide phosphate, NCL: native chemical ligation, NOX3: NADPH oxidase 3, Npys: nitropyridine, PAcBr: phenacyl bromide, PLAD: pre-ligand binding assembly domain, PTM: posttranslational modifications, PS: phosphatidylserine, ROS: reactive oxygen species, RP-HPLC: reversed phase HPLC, rt: room temperature, SAD: self-assembling domain, sFasL: soluble Fas ligand, SGP: sialylglycopeptide, SPPS: solid phase peptide synthesis, tBu: tert butyl, TCEP: tris(2-carboxyethyl)phosphine hydrochloride, TFA: trifluoroacetic acid, THF: tetrahydrofuran, TIPS: triisopropylsilane, TNF: tumor necrosis factor, VGFR: vascular endothelial growth factor receptor.

Supporting information

Additional references cited within the Supporting Information[26p,27–28,34b,39–40]

Acknowledgements

We are grateful for the help of Manuel Felkl, Florian Exler, Margret Vogt and Philipp Schilling with automated peptide synthesis and kindly acknowledge the MS core facility of the Faculty of Chemistry at the University of Vienna for performing high-resolution mass analyses.

Conflict of Interests

The authors declare no conflict of interest.

Data Availability Statement

The data that support the findings of this study are available from the corresponding author upon reasonable request.

Keywords: chemical protein synthesis · ligation · glycosylation · diselenide-selenoester ligation · Fas ligand

[1] a) B. C. Trauth, C. Klas, A. M. Peters, S. Matzku, P. Moller, W. Falk, K. M. Debatin, P. H. Krammer, *Science* **1989**, *245*, 301–305; b) S. Yonehara, A. Ishii, M. Yonehara, *J. Exp. Med.* **1989**, *169*, 1747–1756.
[2] T. Suda, T. Takahashi, P. Golstein, S. Nagata, *Cell* **1993**, *75*, 1169–1178.
[3] a) A. Krippner-Heidereich, P. Scheurich, in *Fas signaling* (Ed.: H. Wajant), Springer, **2006**, pp. 1–12; b) H. Walczak, *Cold Spring Harbor Perspect. Biol.* **2013**, *5*, a008698.
[4] a) D. Bellgrau, D. Gold, H. Selawry, J. Moore, A. Franzusoff, R. C. Duke, *Nature* **1995**, *377*, 630–632; b) B. Lowin, F. Beermann, A. Schmidt, J. Tschopp, *Proc. Natl. Acad. Sci. USA* **1994**, *91*, 11571–11575; c) G. Berke, *Cell* **1995**, *81*, 9–12.
[5] a) A. M. Chinnaiyan, K. O'Rourke, M. Tewari, V. M. Dixit, *Cell* **1995**, *81*, 505–512; b) M. P. Boldin, E. E. Varfolomeev, Z. Pancer, I. L. Mett, J. H. Camonis, D. Wallach, *J. Biol. Chem.* **1995**, *270*, 7795–7798.
[6] a) M. Muzio, A. M. Chinnaiyan, F. C. Kischkel, K. O'Rourke, A. Shevchenko, J. Ni, C. Scaffidi, J. D. Bretz, M. Zhang, R. Gentz, M. Mann, P. H. Krammer, M. E. Peter, V. M. Dixit, *Cell* **1996**, *85*, 817–827; b) F. C. Kischkel, D. A. Lawrence, A. Tinel, H. LeBlanc, A. Virmani, P. Schow, A. Gazdar, J. Blenis, D. Arnott, A. Ashkenazi, *J. Biol. Chem.* **2001**, *276*, 46639–46646; c) M. P. Boldin, T. M. Goncharov, Y. V. Goltsev, D. Wallach, *Cell* **1996**, *85*, 803–815.
[7] F. C. Kischkel, S. Hellbardt, I. Behrmann, M. Germer, M. Pawlita, P. H. Krammer, M. E. Peter, *EMBO J.* **1995**, *14*, 5579–5588.
[8] a) C. Scaffidi, S. Fulda, A. Srinivasan, C. Friesen, F. Li, K. J. Tomaselli, K. M. Debatin, P. H. Krammer, M. E. Peter, *EMBO J.* **1998**, *17*, 1675–1687; b) M. E. Peter, P. H. Krammer, *Curr. Opin. Immunol.* **1998**, *10*, 545–551.
[9] a) J. Dhein, H. Walczak, C. Baumler, K.-M. Debatin, P. H. Krammer, *Nature* **1995**, *373*, 438–441; b) M. E. Peter, A. Hadji, A. E. Murmann, S. Brockway, W. Putzbach, A. Pattanayak, P. Ceppi, *Cell Death Differ.* **2015**, *22*, 549–559.
[10] O. Janssen, J. Qian, A. Linkermann, D. Kabelitz, *Cell Death Differ.* **2003**, *10*, 1215–1225.
[11] M. Schulte, K. Reiss, M. Lettau, T. Maretzky, A. Ludwig, D. Hartmann, B. de Strooper, O. Janssen, P. Saftig, *Cell Death Differ.* **2007**, *14*, 1040–1049.
[12] a) T. Vargo-Gogola, H. C. Crawford, B. Fingleton, L. M. Matrisian, *Arch. Biochem. Biophys.* **2002**, *408*, 155–161; b) A. Fouque, L. Debure, P. Legembre, *Biochim. Biophys. Acta* **2014**, *1846*, 130–141; c) H. Matsuno, K. Yudoh, Y. Watanabe, F. Nakazawa, H. Aono, T. Kimura, *J. Rheumatol.* **2001**, *28*, 22–28; d) M. Kiaei, K. Kipiani, N. Y. Calingasan, E. Wille, J. Chen, B. Heissig, S. Rafii, S. Lorenzl, M. F. Beal, *Exp. Neurol.* **2007**, *205*, 74–81; e) R. Herrero, O. Kajikawa, G. Matute-Bello, Y. Wang, N. Hagimoto, S. Mongovin, V. Wong, D. R. Park, N. Brot, J. W. Heinecke, H. Rosen, R. B. Goodman, X. Fu, T. R. Martin, *J. Clin. Invest.* **2011**, *121*, 1174–1190.
[13] P. Schneider, N. Holler, J. L. Bodmer, M. Hahne, K. Frei, A. Fontana, J. Tschopp, *J. Exp. Med.* **1998**, *187*, 1205–1213.
[14] a) T. Suda, H. Hashimoto, M. Tanaka, T. Ochi, S. Nagata, *J. Exp. Med.* **1997**, *186*, 2045–2050; b) L. A. O'Reilly, L. Tai, L. Lee, E. A. Kruse, S. Grabow, W. D. Fairlie, N. M. Haynes, D. M. Tarlinton, J.-G. Zhang, G. T. Belz, M. J. Smyth, P. Bouillet, L. Robb, A. Strasser, *Nature* **2009**, *461*, 659–663; c) R. Audo, F. Calmon-Hamaty, L. Papon, B. Combe, J. Morel, M. Hahne, *Arthritis Rheuma* **2014**, *66*, 3289–3299; d) P. G. Knox, A. E. Milner, N. K. Green, A. G. Eliopoulos, L. S. Young, *J. Immunol.* **2003**, *170*, 677–685; e) M. Tanaka, T. Itai, M. Adachi, S. Nagata, *Nat. Med.* **1998**, *4*, 31–36.
[15] a) M. Le Gallo, A. Poissonnier, P. Blanco, P. Legembre, *Front. Immunol.* **2017**, *8*, 1216; b) P. Legembre, B. C. Barnhart, M. E. Peter, *Cell Cycle* **2004**, *3*, 1235–1239.
[16] a) M. Umemura, T. Kawabe, K. Shudo, H. Kidoya, M. Fukui, M. Asano, Y. Iwakura, G. Matsuzaki, R. Imamura, T. Suda, *Int. Immunol.* **2004**, *16*, 1099–1108; b) T. Kataoka, R. C. Budd, N. Holler, M. Thome, F. Martinon, M. Irmler, K. Burns, M. Hahne, N. Kennedy, M. Kovacsovics, J. Tschopp, *Curr. Biol.* **2000**, *10*, 640–648.
[17] a) C. Zhang, F. Gao, F. Teng, M. Zhang, *Cell Biochem. Biophys.* **2015**, *71*, 1319–1323; b) M. Fujiwara, H. Suemoto, Y. Muragaki, A. Ooshima, *J. Dermatol.* **2007**, *34*, 99–109; c) L. Biancone, A. D. Martino, V. Orlandi, P. G. Conaldi, A. Toniolo, G. Camussi, *J. Exp. Med.* **1997**, *186*, 147–152.
[18] a) S. P. Cullen, S. J. Martin, *Semin. Cell Dev. Biol.* **2015**, *39*, 26–34; b) T. Mondal, H. Gaur, B. E. N. Wamba, A. G. Michalak, C. Stout, M. R. Watson, S. L. Aleixo, A. Singh, S. Condello, R. Faller, G. S. Leiserowitz, S. Bhatnagar, J. Tushir-Singh, *Cell Death Differ.* **2023**.
[19] Orphanet.
[20] a) T. A. Schweizer, S. Mairpady Shambat, C. Vulin, S. Hoeller, C. Acevedo, M. Huemer, A. Gomez-Mejia, C. C. Chang, J. Baum, S. Hertegonne, E. Hitz, T. C. Scheier, D. A. Hofmaenner, P. K. Buehler, H. Moch, R. A. Schuepbach, S. D. Brugger, A. S. Zinkernagel, *Clin Transl Immunology* **2021**, *10*, e1357; b) S. André, M. Picard, R. Cezar, F. Roux-Dalvai, A. Alleaume-Butaux, C. Soundaramourty, A. S. Cruz, A. Mendes-Frias, C. Gotti, M. Leclercq, A. Nicolas, A. Tauzin, A. Carvalho, C. Capela, J. Pedrosa, A. G. Castro, L. Kundura, P. Loubet, A. Sotto, L. Muller, J.-Y. Lefrant, C. Roger, P.-G. Claret, S. Duvnjak, T.-A. Tran, G. Racine, O. Zghidi-Abouzid, P. Nioche, R. Silvestre, A. Droit, F. Mammano, P. Corbeau, J. Estaquier, *Cell Death Differ.* **2022**, 1–14; c) M. Muraki, *AIMS Med Sci* **2022**, *9*, 98–267.
[21] M. S. Abers, O. M. Delmonte, E. E. Ricotta, J. Fintzi, D. L. Fink, A. A. A. de Jesus, K. A. Zarember, S. Alehashemi, V. Oikonomou, J. V. Desai, S. W. Canna, B. Shakoory, K. Dobbs, L. Imberti, A. Sottini, E. Quiros-Roldan, F. Castelli, C. Rossi, D. Brugnoni, A. Biondi, L. R. Bettini, M. D'Angio, P. Bonfanti, R. Castagnoli, D. Montagna, A. Licari, G. L. Marseglia, E. F. Gliniewicz, E. Shaw, D. E. Kahle, A. T. Rastegar, M. Stack, K. Myint-Hpu, S. L. Levinson, M. J. DiNubile, D. W. Chertow, P. D. Burbelo, J. I. Cohen, K. R. Calvo, J. S. Tsang, H. C. Su, J. I. Gallin, D. B. Kuhns, R. Goldbach-Mansky, M. S. Lionakis, L. D. Notarangelo, *JCI Insight* **2021**, *6*.
[22] H. Xu, Y. Wang, S. Lin, W. Deng, D. Peng, Q. Cui, Y. Xue, *Genom Proteom Bioinform* **2018**, *16*, 244–251.
[23] Z. Luo, Z. Xu, S. Zhuo, K. Jing, Y. Lu, *Biochemical Eng J* **2012**, *62*, 86–91.
[24] C. Bello, S. Wang, L. Meng, K. W. Moremen, C. F. W. Becker, *Angew. Chem. Int. Ed.* **2015**, *54*, 7711–7715.
[25] a) P. Schneider, J. L. Bodmer, N. Holler, C. Mattmann, P. Scuderi, A. Terskikh, M. C. Peitsch, J. Tschopp, *J. Biol. Chem.* **1997**, *272*, 18827–18833; b) J. R. Orlinick, K. B. Elkon, M. V. Chao, *J. Biol. Chem.* **1997**, *272*, 32221–32229.
[26] a) L. F. Mackenzie, Q. Wang, R. A. J. Warren, S. G. Withers, *JACS* **1998**, *120*, 5583–5584; b) C. Li, L.-X. Wang, *Chem. Rev.* **2018**, *118*, 8359–8413; c) A. J. Fairbanks, *Pure Appl. Chem.* **2013**, *85*, 1847–1863; d) M. Umekawa, C. Li, T. Higashiyama, W. Huang, H. Ashida, K. Yamamoto, L. X. Wang, *J. Biol. Chem.* **2010**, *285*, 511–521; e) M. Umekawa, W. Huang, B. Li, K. Fujita, H. Ashida, L. X. Wang, K. Yamamoto, *J. Biol. Chem.* **2008**, *283*, 4469–4479; f) W. Huang, C. Li, B. Li, M. Umekawa, K. Yamamoto, X. Zhang, L. X. Wang, *J. Am. Chem. Soc.* **2009**, *131*, 2214–2223; g) C. D. Heidecke, Z. Ling, N. C. Bruce, J. W. B. Moir, T. B. Parsons, A. J. Fairbanks, *ChemBioChem* **2008**, *9*, 2045–2051; h) R. M. Schmaltz, S. R. Hanson, C.-H. Wong, *Chem. Rev.* **2011**, *111*, 4259–4307; i) A. L. Tarentino, T. H. Plummer, F. Maley, *J. Biol. Chem.* **1972**, *247*, 2629–2631; j) K. Takegawa, S. Yamaguchi, A. Kondo, I. Kato, S. Iwahara, *Biochem. Int.* **1991**, *25*, 829–835; k) K. Takegawa, S. Yamaguchi, A. Kondo, H. Iwamoto, M. Nakoshi, I. Kato, S. Iwahara, *Biochem. Int.* **1991**, *24*, 849–855; l) K. J. Yamamoto, S. Kadowaki, J. Watanabe, H. Kumagai, *Biochem Bioph Res Co* **1994**, *203*, 244–252; m) K. Yamamoto, *J. Biosci. Bioeng.* **2001**, *92*, 493–501; n) A. Kondo, I. Kato, K. Takegawa, M. Tabuchi, S. Yamaguchi, S. Iwahara, *J. Biol. Chem.* **1995**, *270*, 3094–3099; o) M. Noguchi, T. Tanaka, H. Gyakushi, A. Kobayashi, S.-i. Shoda, *J. Org. Chem.* **2009**, *74*, 2210–2212; p) M.

Noguchi, T. Fujieda, W. C. Huang, M. Ishihara, A. Kobayashi, S.-i. Shoda, *Helv. Chim. Acta* **2012**, *95*, 1928–1936; q) M. Fujita, S.-i. Shoda, K. Haneda, T. Inazu, K. Takegawa, K. Yamamoto, *Biochim. Biophys. Acta* **2001**, *1528*, 9–14.
[27] C. Bello, F. Kikul, C. F. Becker, *J. Pept. Sci.* **2015**, *21*, 201–207.
[28] J. S. Zheng, S. Tang, Y. K. Qi, Z. P. Wang, L. Liu, *Nat. Protoc.* **2013**, *8*, 2483–2495.
[29] a) Y. Sohma, T. Yoshiya, A. Taniguchi, T. Kimura, Y. Hayashi, Y. Kiso, *Biopolymers* **2007**, *88*, 253–262; b) Y. Sohma, M. Sasaki, Y. Hayashi, T. Kimura, Y. Kiso, *Chem. Commun.* **2004**, 124–125; c) L. A. Carpino, E. Krause, C. D. Sferdean, M. Schümann, H. Fabian, M. Bienert, M. Beyermann, *Tetrahedron Lett.* **2004**, *45*, 7519–7523; d) S. Dos Santos, A. Chandravarkar, B. Mandal, R. Mimna, K. Murat, L. Saucède, P. Tella, G. Tuchscherer, M. Mutter, *JACS* **2005**, *127*, 11888–11889.
[30] a) C. Marinzi, S. J. Bark, J. Offer, P. E. Dawson, *Bioorgan Med Chem* **2001**, *9*, 2323–2328; b) T. M. Hackeng, J. H. Griffin, P. E. Dawson, *Proc Natl Acad Sci* **1999**, *96*, 10068–10073; c) M. Schrems, A. V. Kravchuk, G. Niederacher, F. Exler, C. Bello, C. F. W. Becker, *Chem. Eur. J.* **2023**, *29*, e202301253.
[31] a) T. Durek, P. F. Alewood, *Angew. Chem. Int. Ed.* **2011**, *50*, 12042–12045; b) N. J. Mitchell, L. R. Malins, X. Liu, R. E. Thompson, B. Chan, L. Radom, R. J. Payne, *J. Am. Chem. Soc.* **2015**, *137*, 14011–14014; c) S. S. Kulkarni, E. E. Watson, B. Premdjee, K. W. Conde-Frieboes, R. J. Payne, *Nat. Protoc.* **2019**, *14*, 2229–2257; d) T. S. Chisholm, S. S. Kulkarni, K. R. Hossain, F. Cornelius, R. J. Clarke, R. J. Payne, *JACS* **2020**, *142*, 1090–1100.
[32] L. Kerul, M. Schrems, A. Schmid, R. Meli, C. F. W. Becker, C. Bello, *Angew. Chem. Int. Ed.* **2022**, *n//a*.
[33] N. Metanis, E. Keinan, P. E. Dawson, *Angew. Chem. Int. Ed. Engl.* **2010**, *49*, 7049–7053.
[34] a) M. Mochizuki, H. Hibino, Y. Nishiuchi, *Org. Lett.* **2014**, *16*, 5740–5743; b) M. Matveenko, S. Hackl, C. F. W. Becker, *ChemistryOpen* **2018**, *7*, 106–110; c) S. Mukherjee, M. Matveenko, C. F. W. Becker, in *Expressed Protein Ligation: Methods and Protocols* (Ed.: M. Vila-Perelló), Springer US, New York, NY, **2020**, pp. 343–358.
[35] L. Kerul, PhD thesis, University of Vienna **2022**.
[36] A. Schmid, C. F. W. Becker, in *Total Chemical Synthesis of Proteins*, **2021**, pp. 437–462.
[37] E. Gasteiger, C. Hoogland, A. Gattiker, S. e. Duvaud, M. R. Wilkins, R. D. Appel, A. Bairoch, in *The Proteomics Protocols Handbook* (Ed.: J. M. Walker), Humana Press, Totowa, NJ, **2005**, pp. 571–607.
[38] T. Kremsmayr, M. Muttenthaler, *Methods Mol. Biol.* **2022**, *2384*, 175–199.
[39] a) Y. Li, J. Liu, Q. Zhou, J. Zhao, P. Wang, *Chinese J Chem* **2021**, *39*, 1861–1866; b) S. S. Kulkarni, E. E. Watson, J. W. C. Maxwell, G. Niederacher, J. Johansen-Leete, S. Huhmann, S. Mukherjee, A. R. Norman, J. Kriegesmann, C. F. W. Becker, R. J. Payne, *Angew. Chem. Int. Ed.* **2022**, *61*, e202200163.
[40] a) A. Schmid, PhD thesis, University of Vienna **2022**; b) B. Sun, W. Bao, X. Tian, M. Li, H. Liu, J. Dong, W. Huang, *Carbohydr. Res.* **2014**, *396*, 62–69.

Manuscript received: January 11, 2024
Accepted manuscript online: February 16, 2024
Version of record online: March 7, 2024